LUND UNIVERSITY

Altered biventricular hemodynamic forces in patients with repaired tetralogy of Fallot and right ventricular volume overload because of pulmonary regurgitation

Sjöberg, Pia; Töger, Johannes; Hedström, Erik; Arvidsson, Per Martin; Heiberg, Einar; Arheden, Hakan; Gustafsson, Ronny; Nozohoor, Shahab; Carlsson, Marcus

LUND UNIVERSITY

PO Box 117
221 00 Lund
+46 46-222 00 00

1 **Title page**

2 **Title**

3 Altered biventricular hemodynamic forces in patients with repaired Tetralogy of Fallot and right

4 ventricular volume overload due to pulmonary regurgitation

5

6 **Authors**

7 Pia Sjöberg[1], Johannes Töger[1,4], Erik Hedström[1,3], Per Arvidsson[1], Einar Heiberg[1,4], Håkan

8 Arheden[1], Ronny Gustafsson[2], Shahab Nozohoor[2], Marcus Carlsson[1]

9

10

11 **Affiliation**

12 1: Lund University, Department of Clinical Sciences, Lund, Clinical Physiology, Skåne

13 University Hospital, Sweden.

14 2: Lund University, Department of Clinical Sciences, Lund, Cardiothoracic Surgery, Skåne

15 University Hospital, Sweden.

16 3: Lund University, Department of Clinical Sciences, Lund, Diagnostic Radiology, Skåne

17 University Hospital, Sweden.

18 4: Lund University, Department of Biomedical Engineering, Faculty of Engineering, Sweden.

19

20 **List of authors contributions**

21   • MC and HA conceived the study.

22   • MC, RG, SN and PS designed the study.

23   • JT and EH developed the methodology.

24   • MC, PA, PS, RG and SN included patients and controls.

25   • PS, PA and MC performed the analysis.

26   • All authors interpreted the results and contributed with intellectual input to the manuscript

27   and approved the final version.

28   •

29   **Running Head**

30   Hemodynamic forces in right ventricular volume overload

31

32   **Address for Correspondence**

33   Marcus Carlsson, Address: Dept of Clinical Physiology, Skåne University Hospital, 221 85 Lund,

34   Sweden. Phone: +4646173989, e-mail: marcus.carlsson@med.lu.se

35

36   **Abstract**

37   Intracardiac hemodynamic forces have been proposed to influence remodeling and be a marker of

38   ventricular dysfunction. We aimed to quantify the hemodynamic forces in repaired tetralogy of

39   Fallot (rToF) patients to further understand the pathophysiological mechanisms as this could be a

40   potential marker for pulmonary valve replacement (PVR) in these patients. Patients with rToF

41   and PR>20% (n=18) and healthy controls (n=15) underwent magnetic resonance imaging (MRI)

42   including 4D-flow. A subset of patients (n=8) underwent PVR and MRI after surgery. Time-

43   resolved hemodynamic forces were quantified using 4D-flow data and indexed to ventricular

44   volume. Patients had higher systolic and diastolic left ventricular (LV) hemodynamic forces

45   compared to controls in the lateral-septal/LVOT ($p=0.011$; $p=0.0031$) and inferior-anterior

46   ($p<0.0001$; $p<0.0001$) directions, which are forces not aligned with blood flow. Forces did not

47   change after PVR. Patients had higher RV diastolic forces compared to controls in the

48   diaphragm-RVOT ($p<0.001$) and apical-basal ($p=0.0017$) directions. After PVR RV systolic

49   forces in the diaphragm-RVOT direction decreased ($p=0.039$) to lower levels than in controls

50   ($p=0.0064$). RV diastolic forces decreased in all directions ($p=0.0078$; $p=0.0078$; $p=0.039$) but

51   were still higher than in controls in diaphragm-RVOT direction ($p=0.046$). In conclusion, patients

52   with rToF and PR had LV hemodynamic forces less aligned with the intraventricular blood flow

53   compared to controls and higher diastolic RV forces along the regurgitant flow direction in the

54   RVOT and that of tricuspid inflow. Remaining force differences in LV and RV after PVR

55   suggest that biventricular pumping does not normalize after surgery.

56

57

58   **New & Noteworthy**

59   Biventricular hemodynamic forces in patients with repaired Tetralogy of Fallot and pulmonary

60   regurgitation were quantified for the first time. Left ventricular hemodynamic forces are less

61   aligned to the main blood flow direction in patients compared to controls. Higher RV forces were

62   seen along the pulmonary regurgitant and tricuspid inflow directions. Differences in forces versus

63 controls remain after pulmonary valve replacement suggesting that altered biventricular pumping

64 does not normalize after surgery.

65

66 **Keywords**

69

Introduction

Patients with pulmonary regurgitation (PR) after repair of Tetralogy of Fallot (rToF) often develop dilatation of the right ventricle (RV) with progressive right ventricular dysfunction (4), decreased exercise capacity (18) and increased risk of ventricular arrhythmias and sudden death (14). Progressive RV dilatation and RV systolic dysfunction are the main current criteria for pulmonary valve replacement (PVR) to alleviate PR and decrease the risk of adverse outcomes (12, 16), (2). However, it is uncertain at what degree of dilatation intervention should be performed(4, 13). To better guide treatment, increased understanding of ventricular remodeling mechanisms and new quantitative measures of ventricular functional impairment after intervention are desirable.

Time-resolved three-dimensional velocity (4D flow) cardiac magnetic resonance imaging (MRI) offers a unique possibility to visualize and quantify intracardiac blood flow and has previously been used in patients with rToF to demonstrate disturbed kinetic energy in both ventricles (23). The 4D flow technique can also be used to quantify hemodynamic forces in the ventricles (1, 10, 11, 25), i.e. the force needed to accelerate the blood.

During systole the myocardium exerts a force to accelerate the blood and during diastole the blood decelerates, which leads to a counterforce in the myocardium (Newton's third law of motion). Patients with rToF have to accelerate a larger RV stroke volume (SV) than controls due to the pulmonary regurgitation volume and often present with right bundle branch block, which might further influence the intraventricular hemodynamic forces.

The hemodynamic forces in the RV have been studied in healthy volunteers and athletes showing a qualitative consistency between groups (1), but it has not been analyzed in patients with rToF.

92 The hemodynamic forces have also been shown to be disturbed in the left ventricle (LV) in

93 patients with dilated cardiomyopathy and left bundle branch block (10, 11, 22). We therefore

94 hypothesized that these disturbances in hemodynamic forces are related to increased wall stress

95 and the development of remodeling also in the RV. Thus, hemodynamic forces may have the

96 potential to help improve timing of PVR.

97 The aim of this study was therefore to quantify the hemodynamic forces in the RV and LV to

98 further understand the pathophysiological mechanisms in patients with rToF and RV volume

99 overload due to PR.

100

101 **Materials and Methods**

102 *Study design*

103 We prospectively included patients with rToF and PR > 20%, diagnosed by previous MRI or

104 echocardiography and without pulmonary stenosis referred for MRI. A subset of patients (n=8)

105 underwent PVR and a follow up MRI scan with 4D flow 6-12 months after surgery, performed

106 using the same protocol and scanner as at baseline. Indications for PVR were PR fraction ≥35%,

107 progressive RV dilatation with RV end-diastolic volume (EDV) ≥150 ml/m^2 and/or symptoms

108 and signs of heart failure. Healthy controls (n=15) were recruited by advertising at the local

109 institution. The controls underwent MRI including the same 4D flow sequence as used in

110 patients. Inclusion criteria for controls were normal ECG and blood pressure <140/90 mmHg, no

111 cardiovascular medication and no medical history of cardiovascular or other systemic disease.

112 The principles of the Helsinki declaration were followed, and the Regional Ethical Review Board

113 in Lund, Sweden approved the study. Written informed consent was obtained from all subjects

114   before participation.

115

116   *Cardiac Magnetic Resonance Imaging*

117   Magnetic resonance images were acquired with the patient in the supine position using

118   retrospective ECG gating, with a 1.5 T Achieva (Philips Healthcare, Best, the Netherlands) or a

119   1.5 T Magnetom Aera (Siemens Healthcare, Erlangen, Germany). The reason for using two

120   different vendors was change of scanners at the hospital during the study.

121   Balanced steady-state free-precession (bSSFP) cine images covering the entire heart were

122   acquired. Two-dimensional (2D) through-plane phase contrast (PC) flow measurements were

123   performed in the ascending aorta in all subjects to quantify the effective stroke volume. In

124   patients, flow in the pulmonary artery was also acquired to quantify the degree of PR and forward

125   pulmonary flow during end-diastole was used to define restrictive RV physiology. On both

126   scanners, validated (6, 17) prototype 4D-flow sequences for research purpose was used to

127   quantify flow in a volume covering the whole heart. Typical imaging parameters are reported in

128   Table 1. 4D-flow was accelerated with parallel imaging (SENSE 2x1 for Philips Achieva and

129   GRAPPA 2x2 for Siemens Aera) and with a temporal segmentation factor (echo train length) of

130   2. Respiratory navigation for 4D flow was used in 7/18 patients, but due to long acquisition time

131   no navigator was used in 11/18 patients. Gadolinium contrast was not given as part of the study

132   protocol but 0.2 mmol/kg was administered in 16/18 patients due to clinical questions of

133   myocardial fibrosis using late gadolinium enhancement (LGE).

134

135   *Image analysis and calculation of hemodynamic forces*

136 The Segment software package (http://segment.heiberg.se) was used for image analysis, with an

137 in vitro and in vivo validated in-house developed module for 4D-flow analysis of hemodynamic

138 forces (25). A validated method for first-order phase background correction (3, 5) and phase

139 unwrapping (in case of high velocities in the right ventricular outflow tract (RVOT)) was

140 performed prior to analysis.

141 Time-resolved delineations of the endocardium in RV and LV in all timeframes were manually

142 drawn and end-diastolic volume (EDV), end-systolic volume (ESV) and SV were calculated. The

143 delineations were transferred to the 4D-flow dataset. Based on the 4D-flow data the pressure

144 gradient g (N) was calculated using the Navier-Stokes equation,

145 $$\boldsymbol{g} = -\rho \frac{\partial \boldsymbol{v}}{\partial t} - \rho(\boldsymbol{v} \cdot \nabla \boldsymbol{v}) + \mu \nabla^2 \boldsymbol{v}$$

146 where $\boldsymbol{v}$ is the velocity (m/s), ρ the density of blood (1.05 g/cm^3) and μ the viscosity (4.0·10^{-3}

147 Ns/m^2). The hemodynamic force was calculated for each time frame of the cardiac cycle by

148 integrating the pressure gradients over the volume of the LV or RV respectively.

149 The hemodynamic force vectors were analyzed in three dimensions. To relate the forces to the

150 anatomy of the heart and the main blood flow directions, a reference system based on the

151 individual ventricle's anatomy was constructed as follows (Figure 1). First, the AV plane was

152 defined in 2, 3 and 4 chamber views and the apical-basal direction was defined as perpendicular

153 to the AV plane. The lateral-septal direction was defined as perpendicular to the apical-basal

154 direction and parallel to the 3-chamber long-axis image plane and the AV plane. The inferior-

155 anterior direction was defined as perpendicular to the other two directions. In the right ventricle

156 the same directions were used, but the transversal directions were denoted septal-freewall and

157 diaphragm-RVOT (right ventricular outflow tract).

158

Analysis of hemodynamic forces

Hemodynamic force data were resampled in time to a common reference heartbeat to display the

average force over time in patients and controls independent of different heart rates (Figure 2).

Root mean square (RMS) analysis was performed in all three directions to facilitate the

comparison between systolic and diastolic forces regardless of whether the force was negative or

positive in relation to the defined direction. RMS of hemodynamic forces was calculated

as $RMS = \sqrt{\frac{1}{N}\sum_{n=1}^{N} f_n^2}$, where N is the number of time frames in the cardiac cycle and f_n is the

force in the timeframe n.

The ratio between transversal (lateral-septal and inferior-anterior) and longitudinal (apical-basal)

forces was computed for the LV to analyze how the forces align with the blood flow. The

anatomy of the RV with inflow at an angle to the outflow prohibits a transverse/longitudinal ratio

to contribute to the understanding of force and flow alignment.

Hemodynamic forces are presented both without normalization ("absolute" values in Newton

(N)), and also indexed to ventricular volume to be able to compare forces independent of heart

size ("indexed" values in Newton/liter (N/l)).

The larger RV stroke volume compared to LV stroke volume results in larger variation of volume

of the RV during the cardiac cycle in rToF. This cause a larger motion of the ventricles compared

to controls and this may influence the measured hemodynamic forces (7, 24). To analyze how

much the potential difference in forces between patients and controls was explained by this

translational ventricular motion, the maximum center of volume motion of the left and right

179 ventricle were calculated for each force direction. The origin of center of volume was identified

180 in enddiastole. The measured forces caused by the ventricular motion were calculated and

181 presented as the proportion (%) of the intraventricular hemodynamic forces. LGE images were

182 visually assessed where contrast enhancement in the RV wall, not including the septum, was

183 considered RV fibrosis.

184

185 *Statistical analyses*

186 Statistical analyses were performed using GraphPad (v6.04, La Jolla, CA, USA). Continuous

187 variables are presented as mean and standard deviation (SD) or median and range. Differences in

188 characteristics, volumes and forces between rToF patients and healthy volunteers were assessed

189 using the Mann-Whitney U test. Differences in forces before and after PVR were evaluated using

190 the Wilcoxon Rank test. Associations between variables were analyzed by Spearman correlation.

191 Results with a p-value <0.05 were considered statistically significant.

192

193

194 **Results**

195 Subject characteristics and volumetric data are summarized in Table 2. All patients had right

196 bundle branch block. PR fraction was in 3/18 patients: 20-29%, 7/18 patients: 30-39% and 8/18

197 patients: ≥40%. Restrictive physiology was present in 13/18 patients. There were only minor

198 tricuspid regurgitation, in one patient 18 % and in the remaining <10%. RV fibrosis was found in

199 13/18 patients, 2/18 had no RV fibrosis and in 2 patients LGE images were not acquired. Patients

200 with rToF had higher heart rates, smaller LVEDV/BSA and higher RV volumes compared to

201   controls. A decrease in global function was seen predominantly for RVEF but LVEF was also

202   lower compared to controls.

203

204   *Qualitative hemodynamic force patterns*

205   The mean hemodynamic force during the cardiac cycle in the three different directions are shown

206   in Figure 2 for patients and controls. In early systole the forces were mainly directed towards the

207   outflow tract and base of the heart in both LV and RV, reflecting the acceleration of blood out of

208   the ventricles. In late systole the forces were reversed, corresponding to the deceleration of blood

209   outflow during late systole. During the first part of early diastolic inflow the forces were directed

210   towards the apex and diaphragm, reflecting acceleration of blood flowing into the ventricles.

211   During the latter part of early diastolic inflow, the forces reversed and were mainly oriented

212   towards the base, reflecting the deceleration of blood entering the ventricle. In patients with rToF

213   and PR there was a continuous hemodynamic force throughout the diastole towards the base and

214   RVOT (Figure 2, Panel C). This continuous RV hemodynamic force during diastole was not

215   present in controls.

216

217   *Quantitative hemodynamic forces - Left ventricle*

218   Patients with rToF and PR had higher RMS of indexed hemodynamic forces in the LV both in

219   systole and diastole in the lateral-septal/LVOT and inferior-anterior directions (Table 3A and

220   Figure 3A and B). Higher absolute hemodynamic forces were found in patients in systole for the

221   inferior-anterior and apical basal directions and in diastole for inferior-anterior direction.

222   The transversal hemodynamic forces in the LV (lateral-septal/LVOT and inferior-anterior)

223   constitute a larger fraction of the total force during systole in patients with rToF compared to

224   controls (Figure 4). The mean ratio of transversal and longitudinal (apical-basal) forces during

225   systole was 1.03 (0.29) in rToF vs 0.72 (0.15) in controls (p=0.0007) and during diastole 0.49

226   (0.20) in rToF vs 0.44 (0.13) in controls (p=0.60).

227

228

229   *Quantitative hemodynamic forces - Right ventricle*

230   In systole, the absolute hemodynamic forces were larger in the diaphragm-RVOT and apical-

231   basal directions in patients compared to controls. No differences were found between patients and

232   controls for indexed hemodynamic forces during systole. In diastole, however, patients with rToF

233   and PR had higher absolute and indexed hemodynamic forces in the diaphragm-RVOT and

234   apical-basal directions (Table 3B, Figure 3C and 3D).

235   There was a moderate to strong positive correlation between PR fraction and RMS of

236   hemodynamic forces in the diaphragm-RVOT direction (systole: r=0.59, p=0.01 and diastole:

237   r=0.53, p=0.024). A strong correlation was also found for PR volume and hemodynamic forces in

238   the diaphragm-RVOT direction (systole: r=0.74, p=0.0005; and diastole: r=0.65, p=0.0036).

239

240   *Effect of PVR*

241   Median follow up time after PVR was 10 months, range 6-21 months. One patient had a later

242   reexamination than planned, 21 months after surgery, due to factors unrelated to the heart

243   condition. RV volumes decreased after surgery but RVEF and LV volumes and LVEF were

244   unchanged (Table 4). After PVR patients still had lower LVEDV/BSA than controls, whereas

245   RVESV and RVESV/BSA remained higher and RVEF lower (Table 2).

246   The effects of PVR on the individual patients' absolute hemodynamic forces are shown in Figure

247   5. To evaluate if the differences after surgery were only related to the change in volumes, the

248   indexed hemodynamic forces are shown in Table 5A and B. The lower forces in the diaphragm-

249   RVOT direction than controls remained also after indexing.

250

251   The intra-individual hemodynamic forces in the LV did not change after PVR (Figure 5), thus the

252   ratio between transversal and longitudinal forces in the LV did not differ before compared to after

253   PVR (systole p=0.64, diastole p=0.74). Patients with rToF after PVR still had higher forces in the

254   inferior-anterior direction of the LV during both systole (0.39 N/ml (0.13)) and diastole (0.49

255   N/ml (0.18)) compared to controls (systole 0.23 N/ml (0.057), p=0.0011; diastole 0.18 N/ml

256   (0.072), p<0.0001) (Figure 6). Patients also still had higher indexed LV hemodynamic forces

257   after PVR in the lateral-septal/LVOT direction during systole compared to controls (1.13 N/ml

258   (0.43) vs 0.65 N/ml (0.34), p=0.019).

259

260   Systolic RV hemodynamic forces in the diaphragm-RVOT direction decreased postoperatively

261   (Figure 5 and Table 5B) resulting in lower forces postoperatively compared to controls (0.75

262   N/ml (0.17) vs 1.02 N/ml (0.29), p=0.0064). During diastole there was a decrease in the RMS of

263   the hemodynamic forces in all directions; septal-freewall (p=0.0078), diaphragm-RVOT

264   (p=0.0078) and apical-basal (p= 0.039) but patients with rToF still after PVR had higher forces in

265   the diaphragm-RVOT direction in diastole compared to controls (0.41 N/ml (0.11) vs 0.27 N/ml

266   (0.12), p=0.046).

267   After PVR the higher LV indexed systolic hemodynamic forces in patients in the transversal

268   planes compared to controls remained. The higher LV diastolic indexed hemodynamic forces in

269   patients in the inferior-anterior direction compared to controls also remained after PVR and there

270   was no difference in diastolic LV forces in the other directions.

271   In contrast to before PVR, the RV indexed systolic hemodynamic forces in the diaphragm-RVOT

272   direction in patients was lower compared to controls after PVR. The higher indexed diastolic

273   hemodynamic forces in the diaphragm-RVOT direction in patients compared to controls

274   remained after PVR but the difference in the apical-basal direction no longer remained. Thus,

275   alterations in hemodynamic forces remained after PVR.

276

277   *Effect of translational ventricular movement on hemodynamic forces*

278   The LV center of volume in patients moved more towards the septum/LVOT and inferiorly

279   during the cardiac cycle than in controls (Table 6A). The proportion of the forces that was caused

280   by LV center of volume motion varied from -14 % to +4 %, with no difference between patients

281   and controls (Table 6B).

282   The RV center of volume had a larger movement towards the RV free wall, but less towards the

283   septum and apex in patients compared to controls (Table 6A). The proportion of the forces that

284   was caused by RV center of volume motion varied from -15 to +10 % (Table 6B). Differences

285   between patients and controls were seen in the diaphragm-RVOT direction in diastole and the

286   apical-basal direction in systole (Table 6A).

287

Discussion

289   This study is the first to quantify intracardiac hemodynamic forces in patients with rToF. The

290   hemodynamic forces were less aligned with the intraventricular blood flow compared to controls

291   in the LV. Higher forces in the RV are seen in patients along the regurgitant flow direction in the

292   RVOT as well as tricuspid inflow. Forces remains altered after PVR indicating that the affected

293   biventricular pumping does not normalize completely after surgery.

294

LV hemodynamic forces

296   The ratio between the transversal and longitudinal forces in the LV was higher in patients with

297   rToF compared to controls, caused by both lower longitudinal forces and higher transversal

298   forces in patients. This means that the main alignment of hemodynamic forces along the

299   longitudinal axis seen in the healthy LV in controls (22) is altered in rToF patients with a small

300   LV and preserved EF. This misalignment of force and flow has also been shown in patients with

301   dilated cardiomyopathy and decreased EF (10). Ventricular dyssynchrony is thought to be one

302   factor causing increased transversal vs. longitudinal hemodynamic forces in dilated

303   cardiomyopathy (11) and might be a contributing factor also in patients with rToF.

304   The increased transversal forces suggest a less efficient LV pumping in patients, since these

305   forces are not aligned with the blood flow. Earlier studies have suggested that the misalignment

306   of intraventricular hemodynamic forces and blood flow activate epigenetic mechanisms leading

307   to pathological cardiac remodeling, possibly through increased wall stress (20, 22). If this

308   hypothesis is correct, one of the major purposes of PVR in patients with rToF and PR would be to

309   realign the hemodynamic forces in the ventricle with the blood flow. In this study LV forces did

310   not change after surgery. This may indicate that the timing of surgery was not optimal and

311   performed too late for completely normalizing blood flow and ventricular pumping.

312   A possible explanation to the higher forces in diastole could be that the LV in rToF has lower

313   preload (19) and the LV has to generate higher forces to fill the ventricle, thereby accelerating the

314   blood more. This is supported by our earlier study showing that patients with rToF have lower

315   kinetic energy in systole, but no difference in diastole compared to controls (23).

316

317   *RV hemodynamic forces*

318   Increased RV hemodynamic forces were seen in the main flow directions in patients and was

319   related to the increased flow volumes due to the pulmonary regurgitation. In diastole there were

320   increased hemodynamic forces towards the RVOT. This can be explained by the continuous

321   inflow to the RV due to the PR leading to a deceleration force in the opposite direction. This is

322   supported by the correlation between PR volume and the hemodynamic forces towards the RVOT

323   during diastole. In the control group there is no PR and thus no deceleration force towards the

324   RVOT.

325   The increased force towards the base during diastole in patients compared to controls, both in

326   absolute and indexed values, is the deceleration force on the inflowing blood from the tricuspid

327   valve. Blood entering a healthy RV is mainly caused by longitudinal lengthening and this does

328   not result in an acceleration of blood and thus no deceleration force (8). In patients with a PR, the

329   systolic longitudinal shortening, and thus also diastolic lengthening, is decreased. As a result

330   inflow of blood caused by radial pumping resulting in diastolic suction may be increased (24).

331   The radial pumping will result in a higher acceleration of blood flow entering the RV and may

332   explain higher forces in the apical-basal direction in patients. Furthermore, diastolic function is

333   decreased in rToF patients (15) and restrictive physiology has been linked to RV fibrosis in this

334   patient group (21). In our patient group 72% of the patients with LGE data had RV fibrosis and

335   72% showed restrictive physiology. Further studies will show if diastolic dysfunction with or

336   without RV fibrosis contribute to the higher forces in the apical-basal direction in patients with

337   rToF.

338   Changes in hemodynamic forces in patients after PVR suggests that the decreased RV volume

339   after surgery is the main cause of the decrease in RV hemodynamic forces. Surprisingly, the

340   systolic diaphragm-RVOT force decreased to a level below the forces of the control population.

341   We hypothesize that this may be explained by decreased myocardial contractility.

342   *Effect of translational ventricular motion on hemodynamic forces*

343   Translational ventricular motion contributes to the hemodynamic forces to equal extent in

344   patients and controls except to RV systolic forces in the apical-basal direction and in RV diastolic

345   forces in the diaphragm-RVOT direction. This translational contribution did not influence the

346   interpretation of the results, as the magnitudes of differences were considerably larger than the

347   magnitudes caused by motion of the ventricles. This result might seem unexpected considering

348   that the LV in rToF patients have a larger net motion towards the RV in systole, but since the

349   force depends on the acceleration and not only the distance traveled, the duration of the motion

350   also important. Thus, translational motion of the ventricles is not likely to be a major confounder

351   when calculating hemodynamic forces in future studies. Based on this the hemodynamic forces in

352   this study are presented as the total force including the minor contribution caused be the motion

353   of the ventricles to facilitate comparison with other studies.

354

Limitations

The study population is small, especially the subgroup after PVR. However, the control group

showed results consistent with previous studies of hemodynamic forces in healthy subjects (1,

10). The larger RV stroke volume compared to LV stroke volume results in larger variation of

volume of the RV during the cardiac cycle in rToF. This cause a larger motion of the ventricles

compared to controls and this may influence the measured hemodynamic forces Intracardiac

blood flow includes vortex formation, and in an ideal symmetric vortex the net vector would be

zero, since the forces from either side of the vortex would each other cancel out. Therefore, the

present hemodynamic force framework will not capture effects of symmetric vortices. However,

the asymmetric anatomy of the heart typically leads to asymmetric vortices resulting in a net

force.

Assessment of ventricular function must always be considered in the light of load-dependency

and hemodynamic forces may also be dependent on pre-load and after-load. There are non-

invasive load independent techniques described for left ventricular diastolic function (9) but to

the best of our knowledge this has not been applied or validated in the right ventricle and

especially not in patients with pulmonary regurgitation. Future studies might reveal if and how

hemodynamic forces are load dependent.

There was a difference in heart rate between patients and controls and possible impact on

hemodynamic forces cannot be ruled out. 4D flow was acquired both with and without

respiratory gating, but the different methods have been shown to be comparable as shown by

Kanski *et al* (17). MR scanners from two vendors were used in the study but a recent validation

376 study showed good agreement of hemodynamic forces between scans with and without

377 respiratory gating and between different vendors (25). However, while agreement is generally

378 good on a group basis, some variability remains. To minimize the potential effect of using two

379 scanners in the study, the same scanner was always used before and after operation. Further, nine

380 patients and nine controls were examined with the Philips scanner and nine patients and six

381 controls with the Siemens scanner.

382 **Conclusion**

383 Patients with repaired Tetralogy of Fallot and pulmonary regurgitation have less alignment of

384 hemodynamic forces and intraventricular blood flow in the left ventricle compared to controls.

385 Higher right ventricular forces are seen in patients along the regurgitant flow direction in the right

386 ventricular outflow tract and that of the tricuspid inflow direction. These altered force patterns

387 remain after pulmonary valve replacement suggesting that the affected biventricular pumping

388 does not normalize completely after surgery. The potential role of hemodynamic forces for

389 treatment evaluation and decision making in rToF can be the aim for future studies.

390

Disclosures

References

1. **Arvidsson PM**, **Töger J**, **Carlsson M**, **Steding-Ehrenborg K**, **Pedrizzetti G**, **Heiberg E**, **Arheden H**. Left and right ventricular hemodynamic forces in healthy volunteers and elite athletes assessed with 4D flow magnetic resonance imaging. *Am J Physiol - Hear Circ Physiol* 312: H314–H328, 2017.

2. **Baumgartner H**, **Bonhoeffer P**, **De Groot NMS**, **De Haan F**, **Deanfield JE**, **Galie N**, **Gatzoulis MA**, **Gohlke-Baerwolf C**, **Kaemmerer H**, **Kilner P**, **Meijboom F**, **Mulder BJM**, **Oechslin E**, **Oliver JM**, **Serraf A**, **Szatmari A**, **Thaulow E**, **Vouhe PR**, **Walma E**, **Vahanian A**, **Auricchio A**, **Bax J**, **Ceconi C**, **Dean V**, **Filippatos G**, **Funck-Brentano C**, **Hobbs R**, **Kearney P**, **McDonagh T**, **Popescu BA**, **Reiner Z**, **Sechtem U**, **Sirnes PA**, **Tendera M**, **Vardas P**, **Widimsky P**, **Swan L**, **Andreotti F**, **Beghetti M**, **Borggrefe M**, **Bozio A**, **Brecker S**, **Budts W**, **Hess J**, **Hirsch R**, **Jondeau G**, **Kokkonen J**, **Kozelj M**, **Kucukoglu S**, **Laan M**, **Lionis C**, **Metreveli I**, **Moons P**, **Pieper PG**, **Pilossoff V**, **Popelova J**, **Price S**, **Roos-Hesselink J**, **Uva MS**, **Tornos P**, **Trindade PT**, **Ukkonen H**, **Walker H**, **Webb GD**, **Westby J**. ESC Guidelines for the management of grown-up congenital heart disease (new version 2010). *Eur Heart J* 31: 2915–2957, 2010.

3. **Bock J**, **Töger J**, **Bidhult S**, **Markenroth Bloch K**, **Arvidsson P**, **Kanski M**, **Arheden H**, **Testud F**, **Greiser A**, **Heiberg E**, **Carlsson M**. Validation and reproducibility of cardiovascular 4D-flow MRI from two vendors using 2x2 parallel imaging acceleration in pulsatile flow phantom and in vivo with and without respiratory gating. *Acta radiol.* (2018). doi: 10.1177/0284185118784981.

4. **Bokma JP**, **Winter MM**, **Oosterhof T**, **Vliegen HW**, **van Dijk AP**, **Hazekamp MG**,

430   **Koolbergen DR**, **Groenink M**, **Mulder BJ**, **Bouma BJ**. Preoperative thresholds for mid-

431   to-late haemodynamic and clinical outcomes after pulmonary valve replacement in

432   tetralogy of Fallot. *Eur Heart J* 37: 1–7, 2015.

433   5.   **Busch J**, **Giese D**, **Kozerke S**. Image-based background phase error correction in 4D flow

434   MRI revisited. *J Magn Reson Imaging* 46: 1516–1525, 2017.

435   6.   **Carlsson M**, **Heiberg E**, **Toger J**, **Arheden H**. Quantification of left and right ventricular

436   kinetic energy using four-dimensional intracardiac magnetic resonance imaging flow

437   measurements. *Am J Physiol Heart Circ Physiol* 302: H893-900, 2012.

438   7.   **Carlsson M**, **Rosengren A**, **Ugander M**, **Ekelund U**, **Cain PA**, **Arheden H**. Center of

439   volume and total heart volume variation in healthy subjects and patients before and after

440   coronary bypass surgery. *Clin Physiol Funct Imaging* 25: 226–233, 2005.

441   8.   **Carlsson M**, **Ugander M**, **Heiberg E**, **Arheden H**. The quantitative relationship between

442   longitudinal and radial function in left, right, and total heart pumping in humans. *Am J*

443   *Physiol Heart Circ Physiol* 293: H636-44, 2007.

444   9.   **Chung CS**, **Shmuylovich L**, **Kovács SJ**. What global diastolic function is, what it is not,

445   and how to measure it. *Am J Physiol Circ Physiol* 309: H1392–H1406, 2015.

446   10.   **Eriksson J**, **Bolger AF**, **Ebbers T**, **Carlhäll C-J**. Assessment of left ventricular

447   hemodynamic forces in healthy subjects and patients with dilated cardiomyopathy using

448   4D flow MRI. *Physiol Rep* 4: e12685, 2016.

449   11.   **Eriksson J**, **Zajac J**, **Alehagen U**, **Bolger AF**, **Ebbers T**, **Carlhäll C-J**. Left ventricular

450   hemodynamic forces as a marker of mechanical dyssynchrony in heart failure patients with

451   left bundle branch block. *Sci Rep* 7: 2971, 2017.

452 12. **Ferraz Cavalcanti PE**, **Sá MPBO**, **Santos CA**, **Esmeraldo IM**, **Escobar RR De**,

453 **Menezes AM De**, **Azevedo OM De**, **Vasconcelos Silva FP De**, **Lins RFDA**, **Lima RDC**.

454 Pulmonary valve replacement after operative repair of Tetralogy of Fallot: Meta-analysis

455 and meta-regression of 3,118 patients from 48 studies. *J Am Coll Cardiol* 62: 2227–2243,

456 2013.

457 13. **Greutmann M**. Tetralogy of Fallot, pulmonary valve replacement, and right ventricular

458 volumes: Are we chasing the right target? *Eur. Heart J*. 37 Oxford University Press: 836–

459 839, 2016.

460 14. **Harrison DA**, **Harris L**, **Siu SC**, **MacLoghlin CJ**, **Connelly MS**, **Webb GD**, **Downar E**,

461 **McLaughlin PR**, **Williams WG**. Sustained ventricular tachycardia in adult patients late

462 after repair of tetralogy of Fallot. *J Am Coll Cardiol* 30: 1368–1373, 1997.

463 15. **Helbing WA**, **Niezen RA**, **Le Cessie S**, **van der Geest RJ**, **Ottenkamp J**, **de Roos A**.

464 Right ventricular diastolic function in children with pulmonary regurgitation after repair of

465 tetralogy of Fallot: volumetric evaluation by magnetic resonance velocity mapping. *J Am*

466 *Coll Cardiol* 28: 1827–35, 1996.

467 16. **Heng EL**, **Gatzoulis MA**, **Uebing A**, **Sethia B**, **Uemura H**, **Smith GC**, **Diller G-PP**,

468 **McCarthy KP**, **Ho SY**, **Li W**, **Wright P**, **Spadotto V**, **Kilner PJ**, **Oldershaw P**, **Pennell**

469 **DJ**, **Shore DF**, **Babu-Narayan S V.** Immediate and Midterm Cardiac Remodeling After

470 Surgical Pulmonary Valve Replacement in Adults With Repaired Tetralogy of Fallot: A

471 Prospective Cardiovascular Magnetic Resonance and Clinical Study. *Circulation* 136:

472 1703–1713, 2017.

473 17. **Kanski M**, **Töger J**, **Steding-Ehrenborg K**, **Xanthis C**, **Bloch KM**, **Heiberg E**,

474 **Carlsson M**, **Arheden H**. Whole-heart four-dimensional flow can be acquired with

475 preserved quality without respiratory gating, facilitating clinical use: a head-to-head

476 comparison. *BMC Med Imaging* 15: 20, 2015.

477 18. **Kempny A**, **Dimopoulos K**, **Uebing A**, **Moceri P**, **Swan L**, **Gatzoulis MA**, **Diller G-P**.

478 Reference values for exercise limitations among adults with congenital heart disease.

479 Relation to activities of daily life--single centre experience and review of published data.

480 *Eur Heart J* 33: 1386–1396, 2012.

481 19. **Kopic S**, **Stephensen SS**, **Heiberg E**, **Arheden H**, **Bonhoeffer P**, **Ersbøll M**, **Vejlstrup**

482 **N**, **Søndergaard L**, **Carlsson M**. Isolated pulmonary regurgitation causes decreased right

483 ventricular longitudinal function and compensatory increased septal pumping in a porcine

484 model. *Acta Physiol* 221: 163–173, 2017.

485 20. **Mann DL**. Basic mechanisms of left ventricular remodeling: the contribution of wall

486 stress. [Online]. *J Card Fail* 10: S202-6, 2004.

487 21. **Munkhammar P**, **Carlsson M**, **Arheden H**, **Pesonen E**. Restrictive right ventricular

488 physiology after Tetralogy of Fallot repair is associated with fibrosis of the right

489 ventricular outflow tract visualized on cardiac magnetic resonance imaging. *Eur Heart J*

490 *Cardiovasc Imaging* 14: 978–985, 2013.

491 22. **Pedrizzetti G**, **Martiniello AR**, **Bianchi V**, **D 'onofrio A**, **Caso P**, **Tonti G**, **D'Onofrio**

492 **A**, **Caso P**, **Tonti G**. Cardiac fluid dynamics anticipates heart adaptation. *J Biomech* 48:

493 388–391, 2015.

494 23. **Sjöberg P**, **Bidhult S**, **Bock J**, **Heiberg E**, **Arheden H**, **Gustafsson R**, **Nozohoor S**,

495 **Carlsson M**. Disturbed left and right ventricular kinetic energy in patients with repaired

496   tetralogy of Fallot: pathophysiological insights using 4D-flow MRI. *Eur. Radiol.* (2018).

497   doi: 10.1007/s00330-018-5385-3.

498 24. **Stephensen S**, **Steding-Ehrenborg K**, **Munkhammar P**, **Heiberg E**, **Arheden H**,

499   **Carlsson M**. The relationship between longitudinal, lateral, and septal contribution to

500   stroke volume in patients with pulmonary regurgitation and healthy volunteers. *Am J*

501   *Physiol Heart Circ Physiol* 306: H895-903, 2014.

502 25. **Töger J**, **Arvidsson PM**, **Bock J**, **Kanski M**, **Pedrizzetti G**, **Carlsson M**, **Arheden H**,

503   **Heiberg E**. Hemodynamic forces in the left and right ventricles of the human heart using

504   4D flow magnetic resonance imaging: Phantom validation, reproducibility, sensitivity to

505   respiratory gating and free analysis software. *PLoS One* 13, 2018.

506

507

Figure Captions

509   **Figure 1**. Spatial reference for hemodynamic forces. A: The atrioventricular (AV) plane was

510   defined in the 2-, 3- and 4-chamber view. B: The apical-basal direction was perpendicular to the

511   AV plane. C: The lateral-septal direction was parallel to the AV plane (perpendicular to the

512   apical-basal direction) and parallel to the 3-chamber long-axis image plane. The inferior-anterior

513   direction was defined as perpendicular to both the apical-basal and lateral-septal planes. D: In the

514   right ventricle the same directions were used, but the transversal directions were renamed septal-

515   freewall and diaphragm-RVOT (right ventricular outflow tract).

516

517   **Figure 2**. Mean hemodynamic forces with 95% CI during the cardiac cycle in patients with

518   repaired Tetralogy of Fallot and pulmonary regurgitation (rToF) (A and C) and controls (B and

519   D). A and B shows data for the left ventricle (LV) and C and D shows the right ventricle (RV). In

520   the LV the hemodynamic forces are mainly directed towards the septum/LVOT and the base

521   when the blood is accelerated during systole and towards the base in diastole when blood entering

522   the ventricle is decelerated. In the RV the hemodynamic forces are mainly directed towards the

523   RVOT and base during systole reflecting the acceleration of the blood and during diastole

524   towards the base due to the deceleration of the blood entering though the tricuspid valve, but in

525   patients with rToF there is also a decelerating force towards the RVOT due to the pulmonary

526   regurgitation volume.

527

528   **Figure 3**. RMS of hemodynamic forces indexed to ventricular volume in patients with repaired

529   Tetralogy of Fallot and pulmonary regurgitation (rToF) and controls. A and B shows the left

530   ventricle (LV), C and D shows the right ventricle (RV). Systolic hemodynamic forces are shown

531   in the left column and diastolic in the right column. Values are presented as mean (SD).

532   In the LV patients with rToF and pulmonary regurgitation (PR) had higher hemodynamic forces

533   in the lateral-septal/LVOT direction and the inferior anterior direction, thus acting un-aligned

534   with the blood flow, than controls in both systole and diastole.

535   In the RV there was no difference between patients with rToF and pulmonary regurgitation and

536   controls in systole. However, in diastole patients had higher decelerating forces on the blood flow

537   from the PR (RVOT direction) and tricuspid valve (basal direction).

538

539   **Figure 4.** Transversal/longitudinal ratio of hemodynamic forces in the LV of patients with

540   repaired Tetralogy of Fallot and pulmonary regurgitation (rToF) and controls. Panel A shows

541   systolic values where patients had higher ratio than controls. Panel B shows diastolic values

542   where there was no difference between the groups.

543

544   **Figure 5.** RMS of hemodynamic forces in patients with repaired Tetralogy of Fallot and

545   pulmonary regurgitation (rToF) before and after pulmonary valve replacement (PVR). Values are

546   presented as mean (SD).

547   There was no difference in hemodynamic forces in the left ventricle (LV) after surgery compared

548   to before. Panel A shows LV forces in systole and Panel B LV forces in diastole.

549   Right ventricular (RV) systolic forces decreased in the diaphragm-RVOT direction, Panel C.

550   There was a decrease in RV forces in all three directions during diastole, Panel D.

551

Figure 6. RMS of hemodynamic forces in patients with repaired Tetralogy of Fallot (rToF) after

pulmonary valve replacement (PVR) compared to controls. Values are presented as mean (SD).

Patients after pulmonary valve replacement (PVR) had higher systolic left ventricular (LV) forces

in the transversal directions (inferior-anterior and lateral-septal/LVOT) and higher diastolic LV

forces in the inferior-anterior direction, compared to controls, Panel A.

Patients after PVR had lower systolic RV forces, but higher RV diastolic forces in the

diaphragm-RVOT direction compared to controls.

559

560

561	**Text tables**

562

563 **Table 1.** Imaging parameters used in the current study

Siemens 1.5 T MAGNETOM Aera

Sequence parameters	bSSFP CINE	2D Flow	4D Flow
Flip angle [°]	70	20	8
TE/TR [ms]	1.2/2.7	2.7/4.9	3.5/5.6
Slice thickness [mm]	8	5	Not applicable
Slice gap [mm]	0	Not applicable	Not applicable
Reconstructed spatial resolution [mm^3]	1.2x1.2x8	1.6x1.6x5	3x3x3
Acquired temporal resolution [ms]	43	29	45
Reconstructed timephases	25	35	40
Gating method	Retrospective ECG	Retrospective ECG	Retrospective ECG
Velocity encoding (VENC) [cm/s]	Not applicable	200	100

Philips 1.5 T Achieva

Sequence parameters	bSSFP CINE	2D Flow	4D Flow
Flip angle [°]	60	15	8
TE/TR [ms]	1.4/2.8	3.0/5.2	3.7/6.3
Slice thickness [mm]	8	6	Not applicable
Slice gap [mm]	0	Not applicable	Not applicable
Reconstructed spatial resolution [mm^3]	1.4x1.4x8	1.2x1.2x6	3x3x3
Acquired temporal resolution [ms]	47	29	50
Reconstructed timephases	30	35	40
Gating method	Retrospective ECG	Retrospective ECG	Retrospective ECG
Velocity encoding (VENC) [cm/s]	Not applicable	200	100

564 bSSFP, balanced steady-state free-precession; 2D, 2-dimensional; 4D, 4-dimensional; TE, echo

565 time; TR, repetition time

566

Table 2. Characteristics and volumetric measurements in patients with repaired tetralogy of

Fallot and pulmonary regurgitation before and after pulmonary valve replacement and controls.

Values are presented as mean (SD).

Mean (SD)	Patients with rToF before PVR (n=18)	Controls (n=15)	P-value rToF before PVR vs Controls	Patients with rToF after PVR (n=8)	P-value rToF after PVR vs Controls
Age (years)	29 (13)	31 (7)	0.13	36 (14)	0.65
Gender (male/female)	11/7	10/5	n/a	6/2	n/a
HR (bpm) at 4D flow acquisition	71 (9)	60 (8)	0.0018	73 (12)	0.0099
BSA (m²)	1.9 (0.2)	1.9 (0.2)	0.78	2.0 (0.2)	0.46
LVEDV (ml)	155 (26)	172 (36)	0.11	155 (24)	0.27
LVEDV/BSA (ml/m²)	82 (11)	91 (14)	0.024	78 (13)	0.017
LVESV (ml)	72 (16)	70 (17)	0.78	64 (13)	0.52
LVESV/BSA (ml/m²)	38 (7)	37 (8)	0.92	32 (6)	0.18
LVEF (%)	54 (6)	60 (6)	0.035	59 (4)	0.69
RVEDV (ml)	291 (67)	192 (41)	<0.0001	228 (40)	0.067
RVEDV/BSA (ml/m²)	153 (24)	101 (13)	<0.0001	114 (19)	0.075
RVESV (ml)	167 (49)	88 (23)	<0.0001	140 (32)	0.0002
RVESV/BSA (ml/m²)	87 (19)	46 (9)	<0.0001	70 (15)	<0.0001
RVEF (%)	43 (6)	55 (6)	<0.0001	39 (5)	<0.0001
PRF (%)	39 (9)	0	<0.0001	0	n/a

rToF, repaired Tetralogy of Fallot; PVR, pulmonary valve replacement; HR, heart rate; BSA,

Body Surface Area; LVEDV, left ventricular end-diastolic volume; LVESV, left ventricular end-

systolic volume; LVEF, left ventricular ejection fraction; RVEDV, right ventricular end-diastolic

573 volume; RVESV, right ventricular end-systolic volume; RVEF; right ventricular ejection

574 fraction; PRF, pulmonary regurgitation fraction

Table 3A: RMS of hemodynamic force in the left ventricle for patients with repaired Tetralogy of Fallot and pulmonary regurgitation

(rToF) and controls in N and N/l. Values are presented as mean (SD).

Force direction		Systole			Diastole		
Mean (SD)		rToF (n=18)	Controls (n=15)	P-value	rToF (n=18)	Controls (n=15)	P-value
Lateral-septal/LVOT	N	0.12 (0.034)	0.098 (0.047)	0.12	0.041 (0.016)	0.033 (0.016)	0.10
	N/l	1.05 (0.44)	0.65 (0.34)	0.011	0.37 (0.15)	0.23 (0.064)	0.0031
Inferior-anterior	N	0.046 (0.029)	0.028 (0.0084)	0.0022	0.045 (0.016)	0.024 (0.012)	0.0005
	N/l	0.43 (0.16)	0.23 (0.057)	<0.0001	0.43 (0.15)	0.18 (0.072)	<0.0001
Apical-basal	N	0.13 (0.035)	0.18 (0.062)	0.025	0.14 (0.045)	0.13 (0.037)	0.56
	N/l	1.16 (0.46)	1.24 (0.42)	0.42	1.19 (0.38)	0.87 (0.17)	0.0075

rToF, repaired Tetralogy of Fallot; LVOT, left ventricular outflow tract

579 **Table 3B**: RMS of hemodynamic force in the right ventricle for patients with repaired Tetralogy of Fallot and pulmonary regurgitation

580 (rToF) and controls in N and N/l. Values are presented as mean (SD).

Force direction		Systole			Diastole		
Mean (SD)		rToF (n=18)	Controls (n=15)	P-value	rToF (n=18)	Controls (n=15)	P-value
Septal-freewall	N	0.079 (0.039)	0.058 (0.019)	0.18	0.058 (0.025)	0.042 (0.012)	0.14
	N/l	0.38 (0.19)	0.40 (0.12)	0.46	0.29 (0.093)	0.29 (0.13)	0.84
Diaphragm-RVOT	N	0.25 (0.089)	0.17 (0.059)	0.0075	0.11 (0.048)	0.040 (0.015)	<0.0001
	N/l	1.04 (0.32)	1.02 (0.29)	0.92	0.52 (0.19)	0.27 (0.12)	<0.0001
Apical-basal	N	0.19 (0.096)	0.13 (0.055)	0.040	0.15 (0.071)	0.079 (0.030)	0.0001
	N/l	0.87 (0.45)	0.79 (0.31)	0.70	0.71 (0.24)	0.49 (0.14)	0.0017

581 rToF, repaired Tetralogy of Fallot; RVOT, right ventricular outflow tract

582

583

Table 4. Volumetric measurements in patients with repaired Tetralogy of Fallot (rToF) before

and after pulmonary valve replacement. Values are presented as mean (SD).

Mean (SD) (n=8)	Before PVR	After PVR	P=value
Left ventricle			
LVEDV (ml)	152 (26)	155 (24)	0.46
LVEDV/BSA (ml/m^2)	77 (10)	78 (13)	0.55
LVESV (ml)	71 (17)	64 (13)	0.20
LVESV/BSA (ml/m^2)	36 (7)	32 (6)	0.20
LVEF (%)	53 (7)	59 (4)	0.11
Right ventricle			
RVEDV (ml)	327 (57)	228 (40)	0.0078
RVEDV/BSA (ml/m^2)	165 (17)	114 (19)	0.0078
RVESV (ml)	192 (43)	140 (32)	0.016
RVESV/BSA (ml/m^2)	97 (13)	70 (15)	0.016
RVEF (%)	42 (5)	39 (5)	0.15

PVR, pulmonary valve replacement; LVEDV, left ventricular end-diastolic volume; LVESV, left

ventricular end-systolic volume; LVEF, left ventricular ejection fraction; RVEDV, right

ventricular end-diastolic volume; RVESV, right ventricular end-systolic volume; RVEF; right

ventricular ejection fraction

590

591   **Table 5A**: RMS of hemodynamic force in the left ventricle for patients with repaired Tetralogy of Fallot and pulmonary regurgitation

592   (rToF) before and after pulmonary valve replacement in N and N/l. Values are presented as mean (SD).

Force direction		Systole			Diastole		
Mean (SD), n=8		**Before PVR**	**After PVR**	**P-value**	**Before PVR**	**After PVR**	**P-value**
Lateral-septal/LVOT	N	0.13 (0.046)	0.13 (0.046)	0.64	0.039 (0.015)	0.035 (0.014)	0.31
	N/l	1.11 (0.63)	1.13 (0.43)	0.84	0.40 (0.17)	0.32 (0.13)	0.11
Inferior-anterior	N	0.050 (0.041)	0.040 (0.011)	0.84	0.045 (0.016)	0.040 (0.011)	0.38
	N/l	0.45 (0.22)	0.39 (0.13)	0.46	0.49 (0.18)	0.43 (0.14)	0.15
Apical-basal	N	0.14 (0.037)	0.15 (0.028)	0.55	0.12 (0.044)	0.12 (0.044)	0.55
	N/l	1.28 (0.62)	1.34 (0.32)	0.64	1.06 (0.44)	1.20 (0.44)	0.38

593   PVR, pulmonary valve replacement; LVOT, left ventricular outflow tract

594

595 **Table 5B**: RMS of hemodynamic force (SD) in the right ventricle for patients with repaired Tetralogy of Fallot and pulmonary

596 regurgitation (rToF) before and after pulmonary valve replacement in N and N/l. Values are presented as mean (SD).

Force direction		Systole			Diastole		
Mean (SD), n=8		Before PVR	After PVR	P-value	Before PVR	After PVR	P-value
Septal-freewall	N	0.087 (0.047)	0.071 (0.035)	0.38	0.067 (0.023)	0.043 (0.011)	0.0078
	N/l	0.35 (0.22)	0.32 (0.14)	0.64	0.30 (0.097)	0.29 (0.093)	0.74
Diaphragm-RVOT	N	0.30 (0.10)	0.13 (0.060)	0.0078	0.13 (0.052)	0.063 (0.013)	0.0078
	N/l	1.12 (0.46)	0.75 (0.17)	0.039	0.58 (0.22)	0.41 (0.11)	0.016
Apical-basal	N	0.20 (0.12)	0.13 (0.047)	0.039	0.18 (0.095)	0.11 (0.41)	0.039
	N/l	0.80 (0.50)	0.65 (0.19)	0.74	0.70 (0.33)	0.64 (0.27)	0.84

597 PVR, pulmonary valve replacement; RVOT, right ventricular outflow tract

598

599

600 **Table 6A**. Maximum center of volume motion of the left and right ventricle during the cardiac cycle. The three directions applied for

601 the calculations have been divided in their two opposite directions for separate values from the origin of center of volume in

602 enddiastole. Values are presented as mean distance in mm (SD).

	Force direction Mean (SD), mm	rToF (n=18)	Controls (n=15)	P-value
Left Ventricle	**Lateral**	0.9 (0.9)	1.0 (0.5)	0.13
	Septal/LVOT	4.4 (1.5)	1.4 (0.9)	<0.0001
	Inferior	4.0 (1.5)	1.9 (0.9)	0.0007
	Anterior	0.9 (0.9)	0.9 (0.5)	0.46
	Basal	1.0 (1.2)	1.1 (2.3)	0.61
	Apical	5.2 (2.5)	5.1 (2.0)	0.82
Right Ventricle	**Freewall**	2.6 (1.7)	0.2 (0.3)	<0.0001
	Septal	0.8 (0.7)	3.0 (1.2)	<0.0001
	Diaphragm	1.3 (1.4)	0.9 (0.8)	0.54
	RVOT	4.1 (2.5)	4.3 (2.6)	0.82
	Basal	1.4 (1.0)	0.3 (0.5)	0.0006
	Apical	3.4 (2.1)	9.8 (2.9)	<0.0001

603 rToF, repaired Tetralogy of Fallot; LVOT, left ventricular outflow tract; RVOT, right ventricular outflow tract

604

605

606 **Table 6B**. Proportion (%) of the calculated hemodynamic forces caused by the center of volume motion of the left and right ventricle.
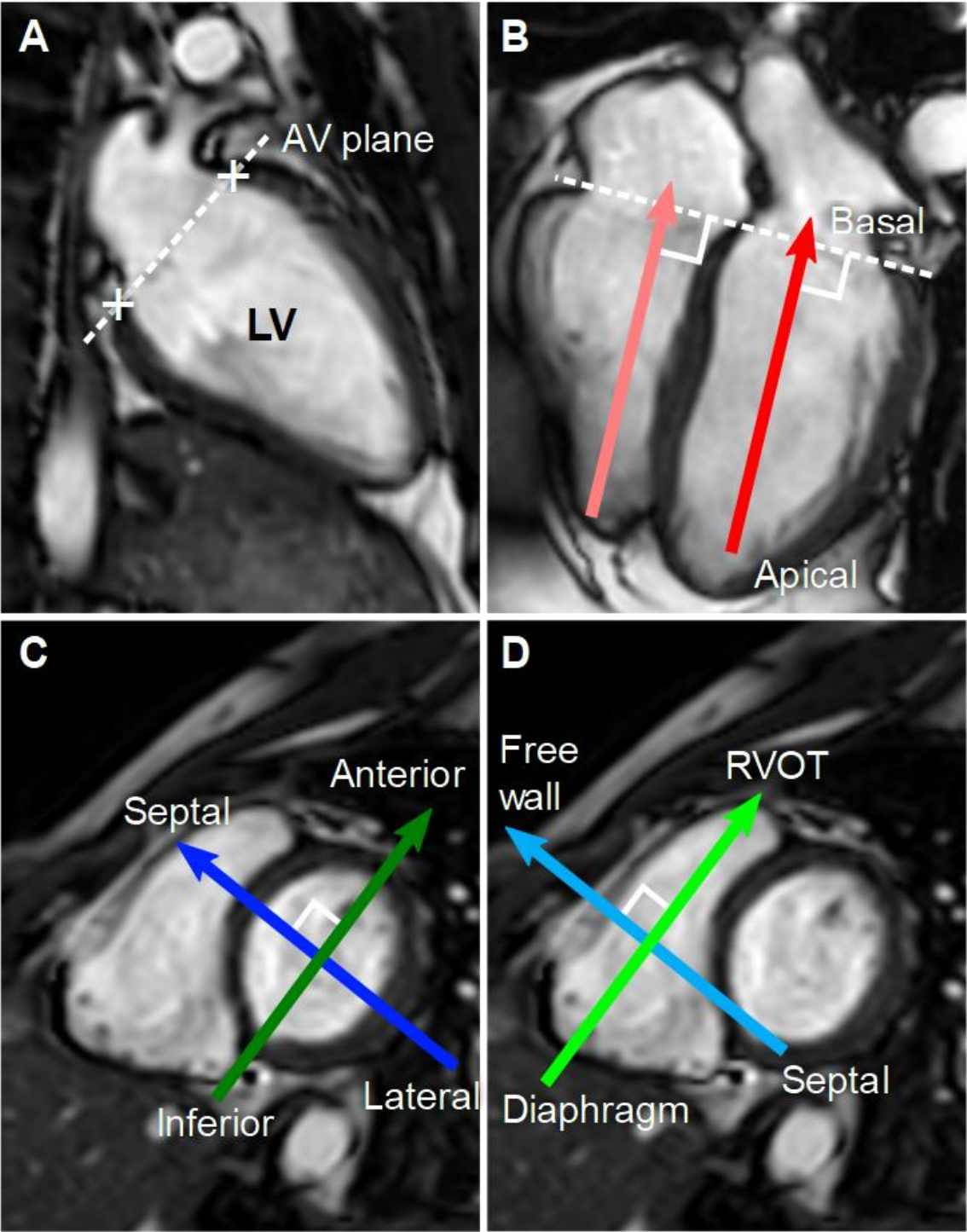
607 Values are presented as mean (SD).

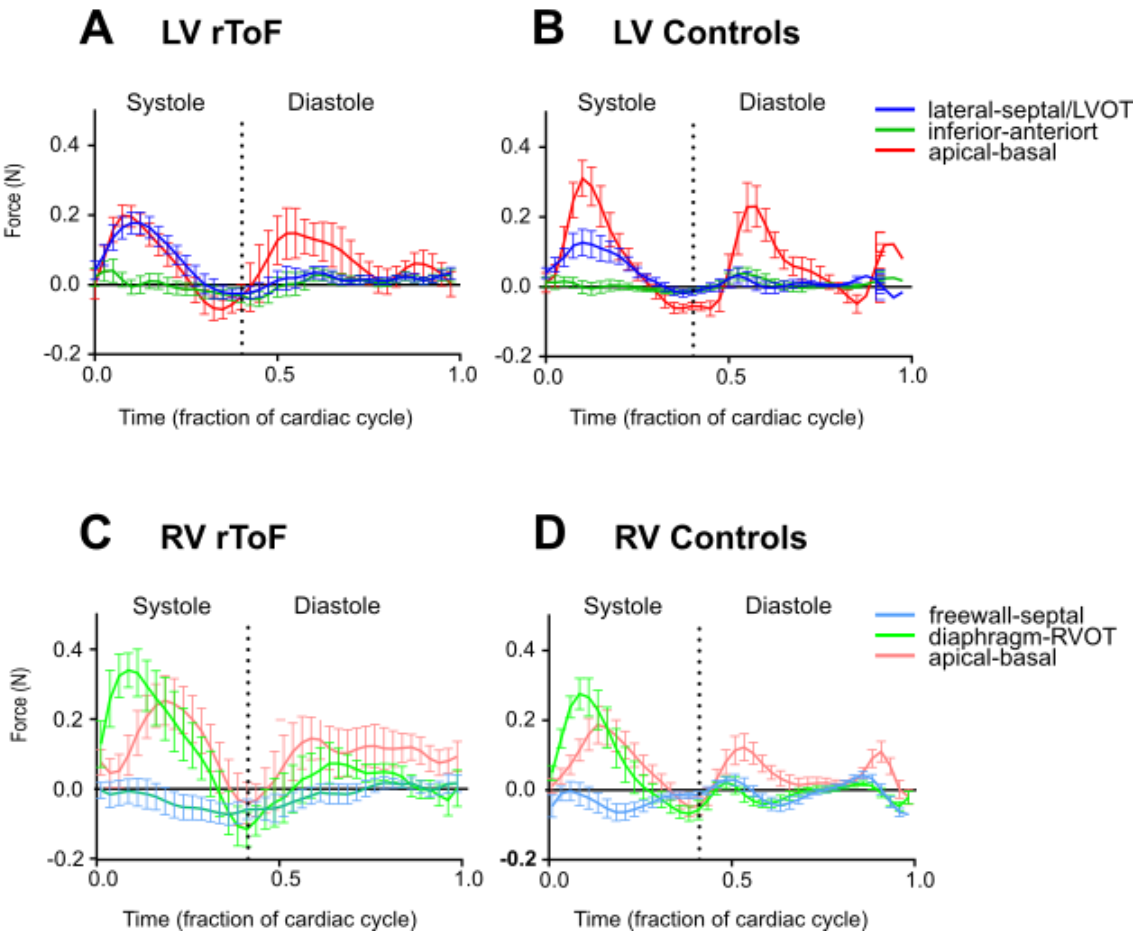|	Force direction	Systole			Diastole		
	Mean (SD)	**rToF**	**Controls**	**P-value**	**rToF**	**Controls**	**P-value**
Left Ventricle	**Lateral-septal/LVOT**	-8 (6)	-7 (8)	0.76	-11 (8)	-9 (14)	0.65
	Inferior-anterior	-14 (16)	-13 (16)	0.68	-9 (12)	-13 (20)	0.63
	Apical-basal	-1 (9)	-4 (11)	0.55	4 (9)	4 (12)	0.94
Right Ventricle	**Septal-freewall**	-5 (16)	-3 (17)	0.88	-15 (11)	-15 (14)	0.85
	Diaphragm-RVOT	9 (7)	10 (11)	0.77	6 (11)	-9 (11)	0.0024
	Apical-basal	0 (5)	6 (16)	0.0078	-6 (10)	-9 (18)	0.55

608 rToF, repaired Tetralogy of Fallot; LVOT, left ventricular outflow tract; RVOT, right ventricular outflow tract
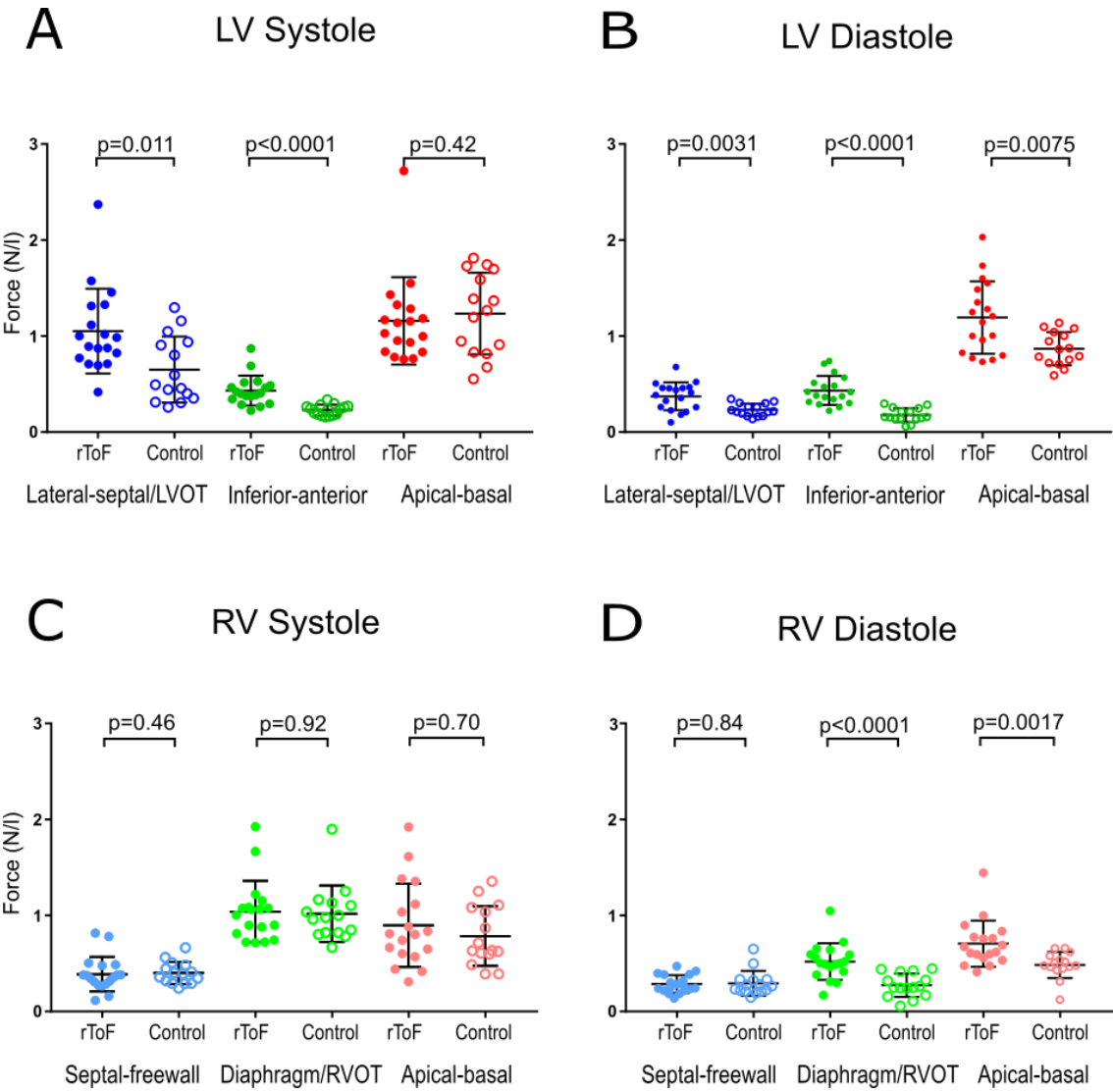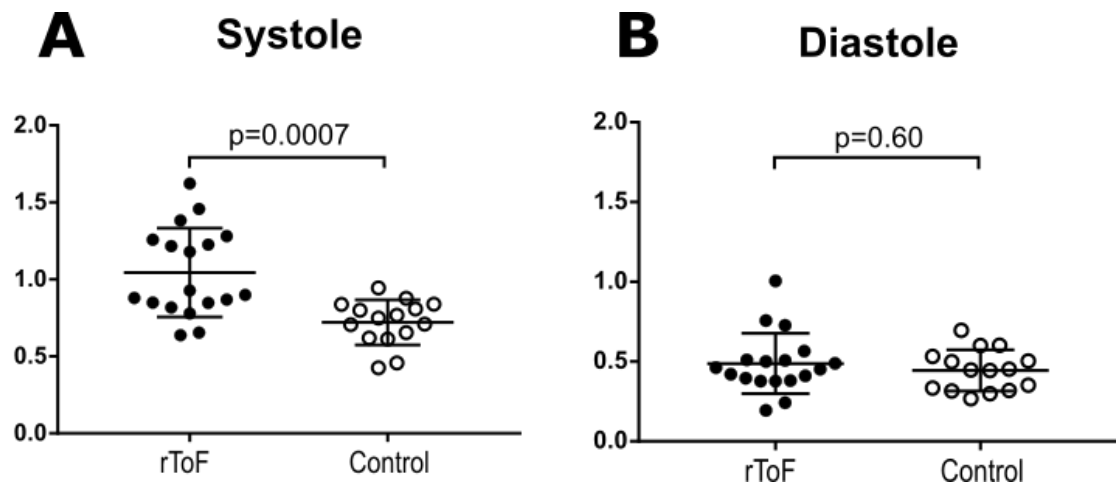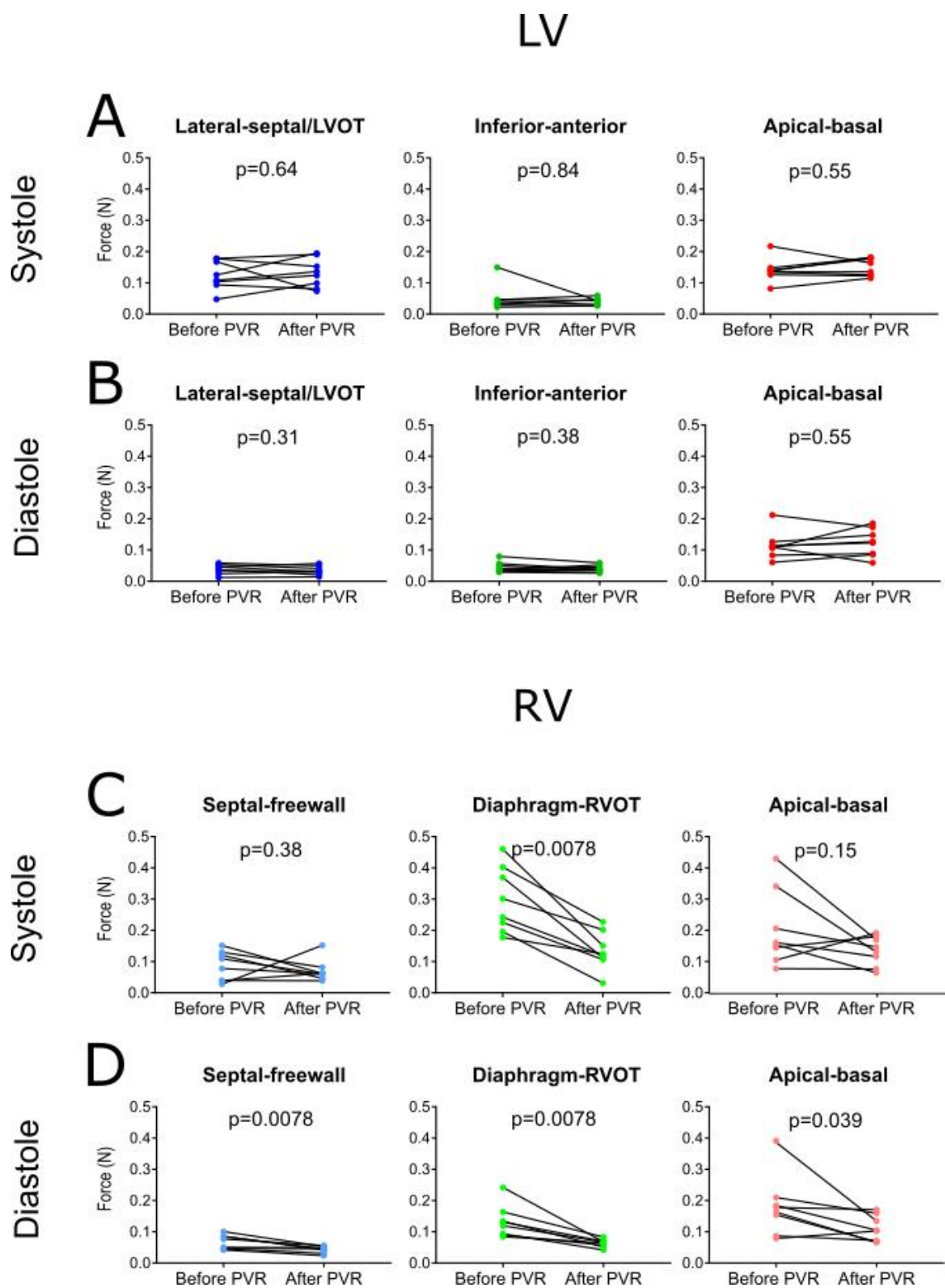
609

610   **Figure 1**

612 **Figure 2**

613

614

Figure 3

619 **Figure 4**

620

621

622

623

624

625 **Figure 5**